JOURNAL OF MATERIALS SCIENCE 25 (1990) 5070–5076

Effect of carbides on the austenite grain growth characteristics in 1Cr–1C and 6Cr–1Mo–1C steels

AMITAVA RAY, SANTANU KR. RAY, S. R. MEDIRATTA
Research and Development Centre for Iron and Steel, Steel Authority of India Limited, Ranchi, 834002, India

The nature of carbides *vis-a-vis* austenite grain growth characteristics in a ball-bearing steel (1Cr–1C) and in a wear-resistant steel (6Cr–1Mo–1C) is reported. Quantitative EPMA analysis was used to determine the type of carbides and *in situ* examination of austenite grain growth was carried out in a hot-stage microscope. The grain size against temperature plots indicated an initial stage of slower "normal" grain growth, followed by the "abnormal" growth, or, grain coarsening beyond a critical soaking temperature. The M_3C type of carbides containing a small amount of chromium could inhibit grain coarsening up to 1223 K in 1Cr–1C steel, whereas the alloy carbides of the M_7C_3 type with a substantial amount (about 35 mass %) of chromium were more effective in restricting grain growth even up to 1273 K in the 6Cr–1Mo–1C steel. In addition, the grain sizes obtained in the latter steel were found to be considerably smaller than those of the former variety at all soaking temperatures investigated.

1. Introduction

Grain size and homogeneity of austenite greatly influence its transformation during cooling to low temperature products and consequently the resulting mechanical properties. This is particularly important in the case of tool steels, which are usually fabricated in the as-annealed condition and subsequently hardened and tempered to obtain the desired hardness and wear resistance. The deleterious effects of high austenitizing temperatures during hardening in conferring inferior strength–toughness combination are well known.

Tool steels in the annealed condition generally consist of discrete carbide particles dispersed in a ferrite matrix. The type and the amount of carbides depend upon the carbon content and the alloying elements present. The process of austenitization involves continuous heating above Ac_{cm} and subsequent soaking at the particular temperature of interest. The transformation during continuous heating comprises the following steps [1]: (i) nucleation of austenite when the temperature exceeds Ac_1, (ii) growth of austenite nuclei prior to impingement, (iii) beginning of carbide dissolution and (iv) growth of austenite grain after impingement, or coarsening. Nucleation and growth of the austenite grains and dissolution of cementite take place within the temperature interval of Ac_1 and Ac_{cm}. At Ac_{cm} cementite is fully transformed and only those carbides, whose dissolution temperatures are higher, remain. Thus impingement of the growing austenite grains is almost complete at this temperature. The composition is, however, still heterogeneous and does not conform to the steel chemistry. Soaking temperatures are, therefore, chosen to be higher than Ac_{cm} to ensure alloying of the austenite for enhanced hardenability as well as to obtain homogeneous austenite. Continued heating above Ac_{cm} up to the soaking temperature entails further growth of the austenite grains after impingement. The grain coarsening behaviour of austenite depends on the type and dispersion of carbide particles present. The final grain size obtained during the process of austenitization is thus influenced by the grain coarsening behaviour *vis-a-vis* the nature of carbides present in the particular grade of steel.

In order to study the effect of carbide nature on austenite grain growth, two alloy steels having almost the same carbon content but different alloying elements were chosen. A typical ball bearing steel (1.0 wt % C, 1.38 wt % Cr, 0.37 wt % Mn, 0.25 wt % Si) and an air-hardenable wear-resistant tool steel (0.90 wt % C, 5.80 wt % Cr, 0.98 wt % Mo, 0.52 wt % Mn, 0.64 wt % Si) in the annealed condition were used in the present study. Although the ball-bearing steel is a standard grade, the wear-resistant 6Cr–1Mo–1C steel was specially made by our research institute and not many scientific data are available for this grade. In spite of the fact that a lot of information on grain growth characteristics of different grades of steel is available, not many direct studies correlating the type of carbides, present in as-annealed tool steels, with their austenitic grain growth behaviour have been undertaken. Moreover, it may be added that the experimental techniques used in the present investigation, namely, (i) quantitative electron-probe microanalysis for identification of the chemistries and the

0022–2461/90 $03.00 + .12

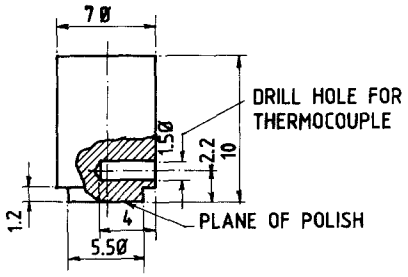

Figure 1 Hot stage sample geometry (all dimensions in mm).

type of carbides, and (ii) hot-stage microscopy for *in situ* observation of "actual" austenite grains at different temperatures, have not been commonly used for such studies.

2. Experimental techniques

2.1. Carbide identification

Quantitative analysis of carbides was carried out in a JCXA-733 computer-controlled electron probe microanalyser (EPMA). The analyses were performed under the condition of an accelerating voltage of 15 kV and a beam current of 5.5×10^{-8} A. A PACM software programme developed by M/s JEOL, Japan employing ZAF correction was used to correct the raw X-ray intensity data for each element. The type of the carbide particles was then determined from the ZAF-corrected analyses.

Visual observation of the analysed carbides was carried out under secondary electron and back-scattered topography modes. Additionally, X-ray mapping images were also observed to study elemental distribution in the carbides.

2.2. *In situ* observation of austenite grains

A number of techniques are available for revealing austenite grain boundaries. McQuaid–Ehn carburization [2], etching by picric acid [3, 4], oxidation [5], delineation by excess ferrite or cementite [6] and thermal etching in vacuum or hot-stage microscopy [7] are some of the common methods which have been used over the years. Most of these methods, however, involve the determination of grain size at a preselected temperature (1198 or 1203 K), rather than revealing the austenite grain at any given temperature. Since the "actual" austenite grain size at the particular austenitizing temperature ultimately dictates the final properties upon cooling, the determination of the "actual" grain size at the temperature of interest is all the more plausible.

The method of revealing austenite grain boundaries through the use of hot-stage microscopy has been chosen in the present investigation for its obvious advantage of *in situ* observation of "actual" austenite grain size at different temperatures.

Samples for hot-stage microscopy were machined in the form of a stepped cylinder shown in Fig. 1. A hole of 1.5 mm diameter was drilled into the sample body to facilitate the insertion of a thermocouple tip for temperature measurement. The bottom face of the sample was polished conventionally and ultrasonically cleaned prior to examination in a Reichert-Vacutherm hot-stage microscope. The heating stage was initially evacuated to 6×10^{-3} Pa and then the heating was commenced. In order to examine *in situ* austenite grain formation and subsequent growth, individual polished and unetched samples were chosen for each soaking temperature. Each such sample was raised to a particular soaking temperature, soaked for 3.6 ksec and a photograph of "actual" austenite grains thus formed at that particular temperature was taken at 100 × magnification. It is well known that at high temperatures under vacuum, the delineation of grain boundaries occurs due to thermal etching, which is basically attributed to higher rate of evaporation from the grain boundaries than that of the grain surfaces. Visual observation was carried out through a round quartz window fitted at the bottom of the heating stage.

2.3. Measurement of austenite grain size

The measurement of austenite grain size was carried out by the linear intercept method on hot-stage micrographs taken at 100 × magnification. For greater measurement accuracy, the number of grains intercepted by twenty random lines, drawn on each micrograph were counted. The average grain diameter D was then determined according to the equation

$$D = \frac{L}{NM}$$

where L is the length of line, N the number of grains intercepted, and M the magnification on the micrograph.

3. Results and discussion

3.1. Carbides in as-annealed structure

The ball bearing steel sample was polished and etched in 4% picral solution to reveal the microstructure. The carbide particles in the spheroidized annealed ball bearing steel were in the form of small spheroids uniformly dispersed in the ferrite matrix. A typical secondary electron image at 2000 × is shown in Fig. 2a. The corresponding back-scattered image showing topographic contrast is given in Fig. 2b. It is apparent that the hard globular carbide particles stand out in relief against the softer matrix. X-ray mapping image of chromium indicating its distribution in the carbide particles as well as in the matrix is shown in Fig. 2c. It is evident that the carbide particles are rich in chromium in comparison to the matrix.

The 6Cr–1Mo–1C wear resistant steel sample was polished and etched in Villela's reagent for microstructural examination. In this case, however, massive skeleton-like carbides along with small finely dispersed carbides were visible. A secondary electron image and the corresponding back scattered topography image of a typical massive carbide particle at 2000 × magnification are shown in Figs 3a and 3b, respectively. Here also, the hard carbide particle appears in relief with respect to the softer matrix. Elemental distribution of chromium and iron are depicted respectively in Figs 3c and 3d. Chromium enrichment and iron depletion are clearly evident from these X-ray mapping images.

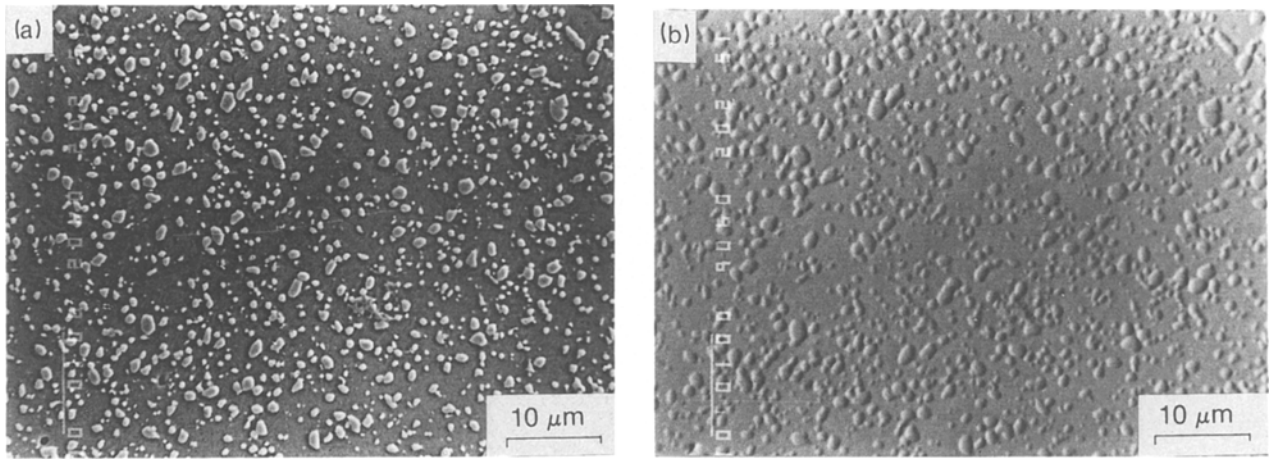

Figure 2 Globular carbides in spheroidized annealed 1Cr–1C ball bearing steel (a) secondary electron image (b) back scattered electron topography image (c) chromium X-ray mapping.

Quantitative analysis employing ZAF correction indicated that the carbide particles are of M_3C type in the 1Cr–1C ball bearing steel and of M_7C_3 type in the 6Cr–1Mo–1C steel. Typical microprobe analyses for each case are shown in Table I. It is evident that iron is replaced by chromium only to a limited extent (about 2 mass or atom %) in the M_3C type carbide of ball bearing steel. In contrast, the M_7C_3 type of carbide in the 6Cr–1Mo–1C steel contains a substantial

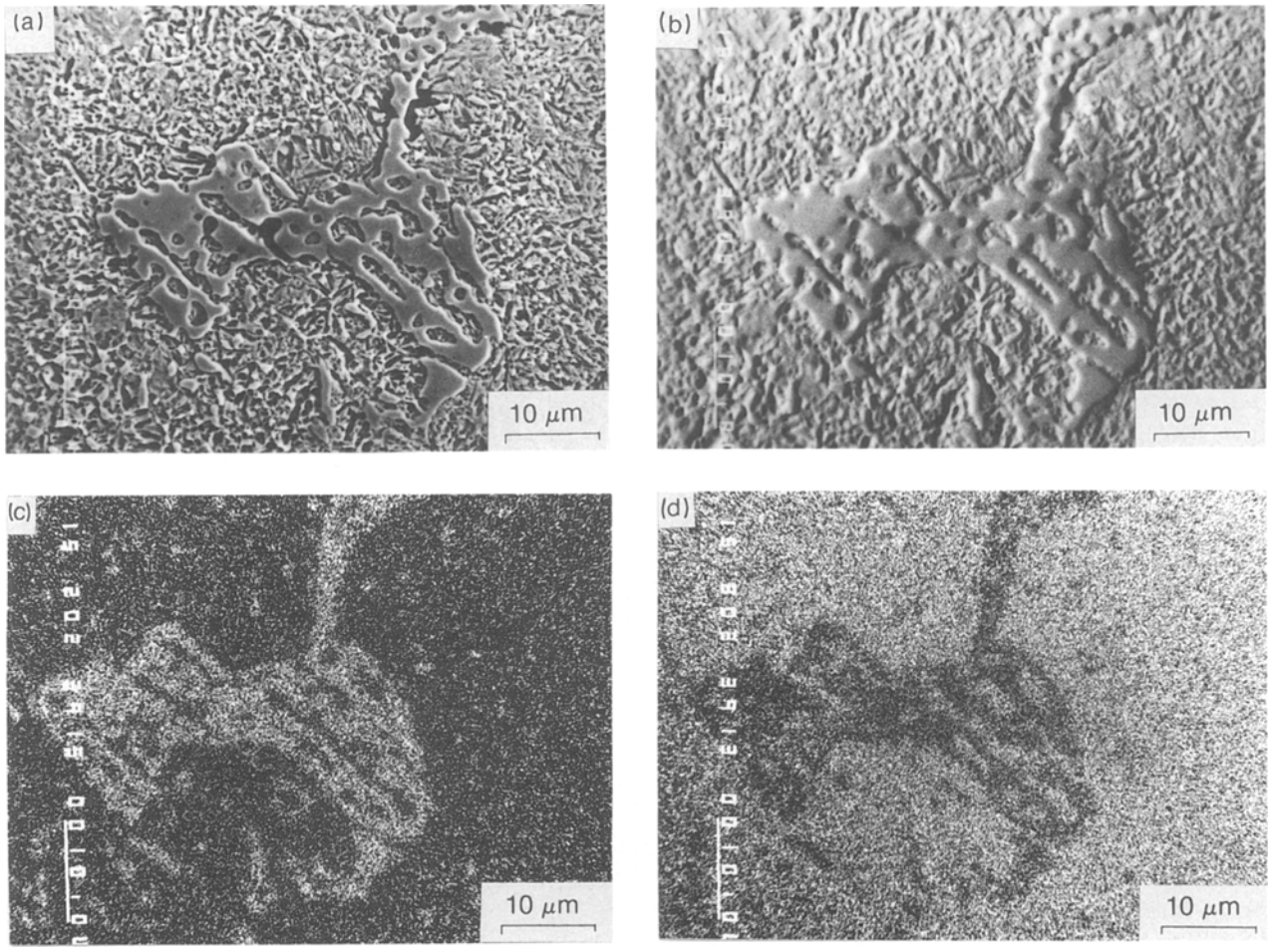

Figure 3 Massive carbide in annealed 6Cr–1Mo–1C steel (a) secondary electron image (b) back scattered electron topography image (c) chromium X-ray mapping (d) iron X-ray mapping.

TABLE I Typical microprobe analyses of (a) M_3C and (b) M_7C_3 carbides

Element	Conc (%)	Atom (%)	K (%)	ZAF	Z	A	F
ICr–IC ball bearing steel							
C	7.286	26.552	2.737	2.6624	0.8255	3.2250	1.0000
Fe	90.092	70.598	88.223	1.0212	1.0193	1.0018	1.0000
Cr	2.804	2.360	3.430	0.8175	1.0204	1.0046	0.7975
Mn	0.607	0.484	0.584	1.0400	1.0388	1.0012	1.0000
Mo	0.013	0.006	0.010	1.2299	1.1083	1.1114	0.9985
	100.802	100.000	94.984	(PACI)	(PH-TX)		
6Cr–1Mo–1C wear resistant steel							
C	8.971	32.928	3.175	2.8254	0.8240	3.4288	1.0000
Fe	41.701	32.914	39.494	1.0559	1.0169	1.0383	1.0000
Mn	0.904	0.725	0.867	1.0421	1.0363	1.0056	1.0000
Cr	34.702	29.417	35.757	0.9705	1.0180	1.0102	0.9438
V	0.112	0.097	0.110	1.0162	1.0369	1.0170	0.9637
Mo	8.529	3.919	7.217	1.1818	1.1056	1.0710	0.9981
	94.919	100.000	86.620	(PACI)	(PH-TX)		

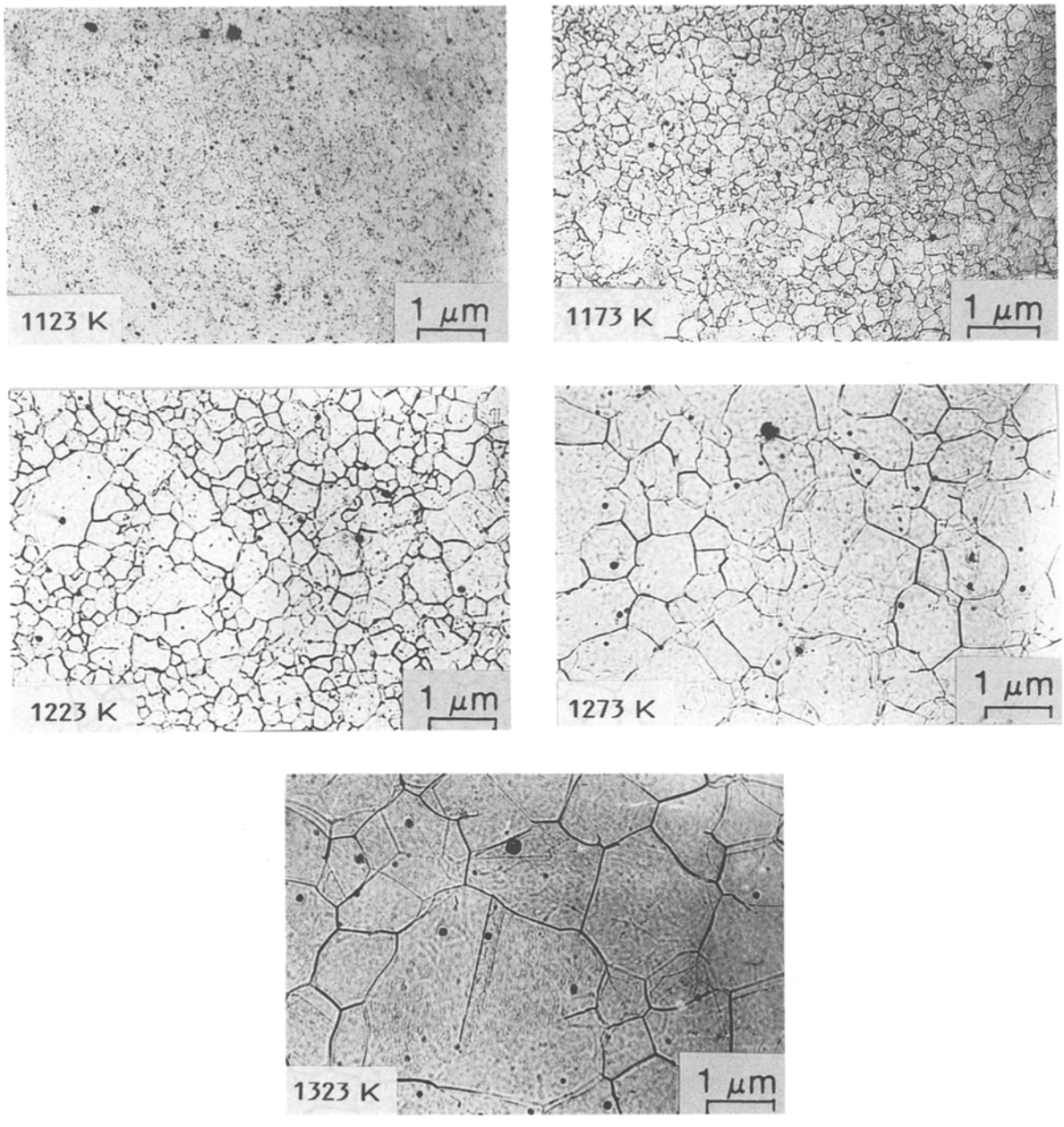

Figure 4 Hot-stage micrographs of 1Cr–1C ball bearing steel showing austenite grains at different soaking temperatures.

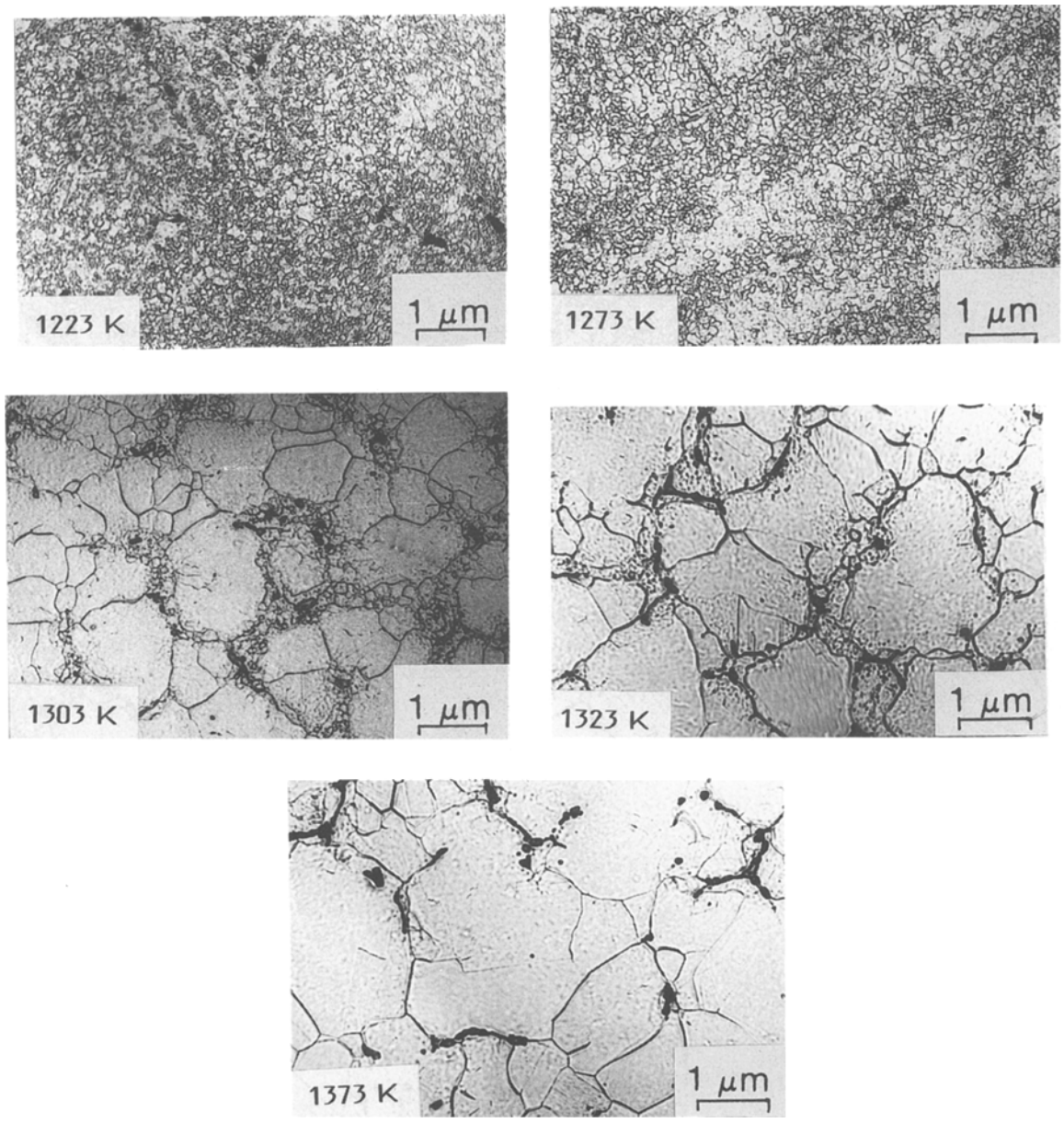

Figure 5 Hot-stage micrographs of 6Cr–1Mo–1C wear resistant steel showing austenite grains at different soaking temperatures.

amount (about 35 mass %) of chromium. This is also borne out from the chromium and iron X-ray images (Figs 3c and 3d) of the M_7C_3 type of carbide in this steel.

The importance of ZAF correction technique in computing the concentration of a lighter element, like carbon, is clearly evident from the significant ZAF correction factor, namely, 2.6624 (for M_3C carbide in 1Cr–1C steel) and 2.8254 (for M_7C_3 carbide in 6Cr–1Mo–1C steel), with which the raw relative intensity, K, is multiplied to obtain the mass fraction.

3.2. Grain growth characteristics

Hot-stage micrographs of the 1Cr–1C ball-bearing and the 6Cr–1Mo–1C steels indicating austenite grains after 3.6 ksec at each soaking temperature are shown in Figs 4 and 5 respectively. The corresponding plots of average austenite grain size at different soaking temperatures are given in Figs 6 and 7.

Austenite grain size increases slowly to the size of 35 μm in the ball bearing steel up to 1223 K, after which increased grain growth is evident. Similarly, in the 6Cr–1Mo–1C steel the grain growth is marginal up to a soaking temperature of 1273 K, above which austenite grains are found to grow to a large extent. Although the pattern of grain growth in both the steel grades is qualitatively similar, finer grain size is obtained at all soaking temperatures for the 6Cr–1Mo–1C steel as compared to the 1Cr–1C ball bearing steel.

An interesting feature is evident from the hot-stage micrograph for the 6Cr–1Mo–1C steel at 1303 K soaking. A few grains were found to have grown abnormally though other grains retained their finer size. This stage is considered as the onset of "abnormal" or "discontinuous" grain growth [8]. In the initial stage of "normal" grain growth, the general distribution of austenite grain size and/or shape remains more or less constant throughout the specimen and only the average size registers slower growth. In contrast, a non-uniform distribution of grain size and/or shape is developed in the next stage of abnormal grain growth, with a relatively small number of grains growing much more rapidly than others. Finally, the

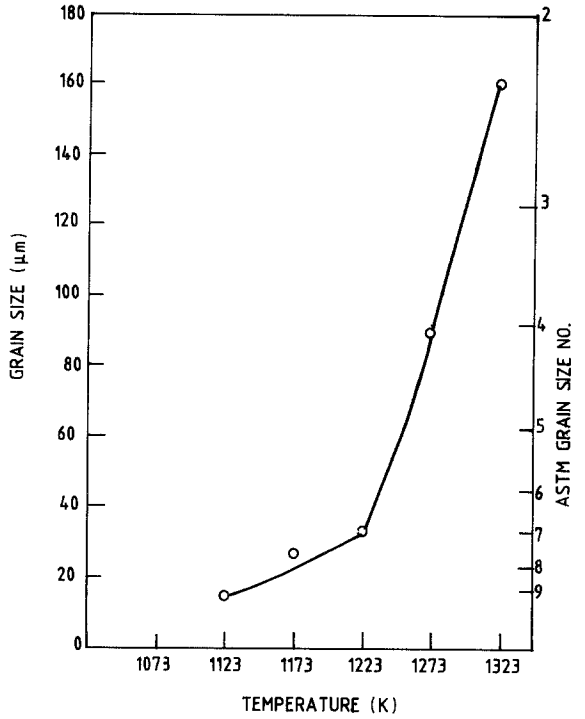

Figure 6 Grain size variation with soaking temperature for 1Cr–1C ball bearing steel.

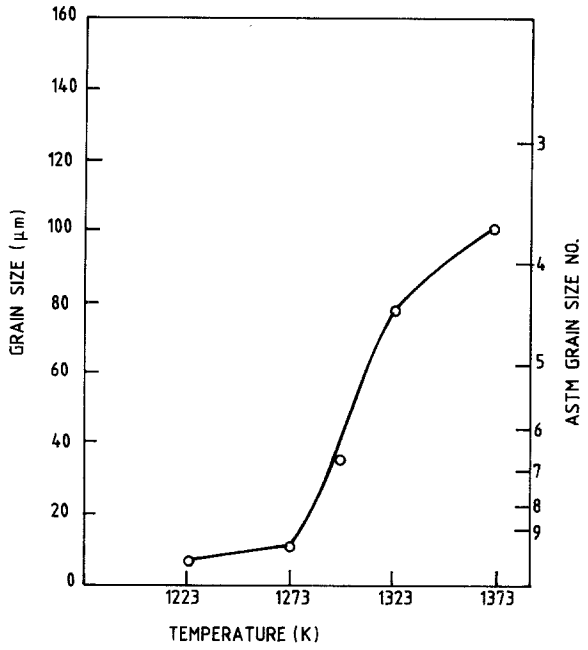

Figure 7 Grain size variation with soaking temperature for 6Cr–1Mo–1C wear resistant steel.

slower-growing bulk of the grains are consumed by the faster-growing grains. It is clear from the hot-stage micrograph of 1323 K soaking that only a few slower-growing grains are still available, which are subsequently consumed at 1373 K. This sequence is similar to the generalized experimental observations of Cahn [9].

3.3. Carbide nature *vis-a-vis* grain growth inhibition

It is well known that the growth of austenite grains in steel is restricted by fine particles of oxides [10], nitrides [11], carbides [12, 13] etc., which act as barriers to grain boundary migration. The problem of the pinning of grain boundaries by second phase particles has been exhaustively treated by Zenner [14] and Paranjpe [15]. In the event of a precipitate lying in the plane of a grain boundary, the missing segment of the boundary has to be created when the boundary moves away from the particle. Energy requirement for the creation of new boundary segment is obviously responsible for the impediment of grain boundary migration in the presence of such fine particles.

In the present study hot-stage microscopy was performed on polished and unetched samples. Conventionally etching is not resorted to in hot stage microscopy because etching residues can lead to reduction in vacuum in the heating stage and additionally the etching film may conceal the finer microstructural details developed at high temperature. In hot-stage microscopy observation of microstructures at high magnifications is not possible owing to working distance limitation. To protect the optical system from the heat, it is essential to employ objectives with long working distance and hence examinations only at low magnifications are possible. The hot-stage micrographs depicted at 100 × magnification show only the austenite grain structure. The carbide particles are not revealed because samples were unetched and observations were done at low magnification. Examination of the polished and etched microstructures, however, at high magnification in EPMA indicated the predominance of M_3C and M_7C_3 type of carbides in the ball bearing and wear resistant grades, respectively.

The nature of the austenite grain size against temperature plots for the two grades of steel under investigation, the slower rise and then the sudden grain coarsening above a certain temperature (1223 K for the ball bearing grade or 1273 K for the wear resistant grade), clearly indicates the marked influence of the respective carbide particles in effecting initial grain growth inhibition. Normally, the carbide particles during the heating process dissolve over a range of temperatures. Not much quantitative information on the rate of solution of different alloy carbides in austenite is available. It is, however, broadly accepted that partial replacement of iron by carbide forming elements, like vanadium, tungsten, molybdenum and chromium in the carbides, tends to retard their solution in austenite [16]. The presence of slight chromium in M_3C type of carbide in the 1Cr–1C ball bearing steel can be thought to be responsible in resisting its dissolution till higher soaking temperatures [17], as compared to simple cementite (Fe_3C) in plain carbon steels. This is possibly instrumental in restricting austenite grain growth in the ball bearing steel up to about 1223 K. The M_7C_3 type alloy carbide, containing about 35 mass % chromium, in the 6Cr–1Mo–1C steel is more effective in inhibiting austenite grain growth till higher soaking temperature (1273 K). Such a carbide is known to go into solution only at still higher temperature [17] in comparison to the M_3C type of carbide with leaner chromium content.

4. Summary

Second phase particles inhibit "normal" austenite grain growth and sudden "abnormal" grain coarsening takes place at higher soaking temperature after the

dissolution of such constituents. The grain coarsening temperature of a heat treatable high carbon steel is thus influenced by the type of carbides present. The M_3C type of carbide with a small amount of chromium is found to restrict grain coarsening in 1Cr–1C steel up to 1223 K. The M_7C_3 type of alloy carbide, however, containing a substantial amount (about 35 mass %) of chromium, present in the 6Cr–1Mo–1C steel is not only effective in inhibiting austenite grain growth up to 1273 K but also helps to maintain finer grain size at all temperatures.

Acknowledgement

The authors are grateful to the management of RDCIS, SAIL, Ranchi for their encouragement and kind permission to publish the paper.

References

1. H. W. PAXTON, "Transformation and Hardenability of Steel" (Climax Molybdenum Company, Michigan, 1977), p. 5.
2. ASTM, Designation E 112-74.
3. P. R. KRAHE and M. GUTTMAN, *Metallography* 7 (1974) 5.
4. A. BROWNRIGG, P. CURCIO and R. BOELEN, *ibid.* **8** (1975) 529.
5. O. O. MILLER and M. J. MAY, *Met. Prog.* **56** (1949), 693.
6. R. MILLSOP, "Hardenability Concepts with Applications to Steel" (AIME, Warrendale, 1978), p. 324.
7. H. MODIN and S. MODIN, "Metallurgical Microscopy" (Butterworths, London, 1973), p. 181.
8. C. A. STICKELS and C. M. YEN, *Trans. AIME* **242** (1968) 833.
9. R. W. CAHN, "Physical Metallurgy" (North-Holland, Amsterdam, 1970).
10. J. HOWARD, *Trans. AIME* **233** (1966) 1791.
11. D. HALL and G. H. J. BENNETT, *J.I.S.I.* **205** (1967) 309.
12. R. PHILIPS and J. A. CHAPMAN, *ibid.* **204** (1966) 615.
13. I. CLASS and G. BOHM, *Archives Eisenhuttenwes* **37** (1966) 67.
14. C. S. SMITH, *Trans. AIME* **175** (1948) 15.
15. V. P. PARANJPE, *Trans. IIM* **6** (1952) 203.
16. G. A. ROBERTS and R. A. CARY, "Tool Steels", 4th edn (ASM, Ohio, 1980), p. 205.
17. Y. GELLER, "Tool Steels" (MIR, Moscow, 1978), p. 187.

Received 31 August 1988
and accepted 1 November 1989